Pressure-induced Fe↔Cu cationic valence exchange and its structural consequences: High-pressure studies of delafossite $CuFeO_2$

W. M. Xu,[1] G. Kh. Rozenberg,[1] M. P. Pasternak,[1] M. Kertzer,[1] A. Kurnosov,[2] L. S. Dubrovinsky,[2] S. Pascarelli,[3] M. Munoz,[3] M. Vaccari,[3] M. Hanfland,[3] and R. Jeanloz[4]

[1]*School of Physics and Astronomy, Tel-Aviv University, Ramat-Aviv, 69997 Tel Aviv, Israel*

[2]*Bayerisches Geoinstitut, University Bayreuth, D-95440 Bayreuth, Germany*

[3]*European Synchrotron Radiation Facility, BP 220, 38043 Grenoble, France*

[4]*Department of Earth and Planetary Science, University of California, Berkeley, California 94720, USA*

(Received 20 August 2009; revised manuscript received 28 October 2009; published 17 March 2010)

The present high-pressure studies of $CuFeO_2$ to 30 GPa using x-ray diffraction, along with ^{57}Fe Mössbauer and Fe and Cu *K*-edge x-ray absorption spectroscopy methods, reveal a sequence of intricate structural/electronic-magnetic pressure-induced transitions. The low-pressure $R\bar{3}m$ structure (0–18 GPa) is composed of sheets of $Fe^{3+}_{S=5/2}$ ions alternating with layers of O-$Cu^{1+}_{S=0}$-O dumbbells, the latter oriented along the *c* axis. This structure is characterized by an unusual positive $d(c/a)/dP$. At 18 GPa a structural transition takes place to a more isotropic $C2/c$ structure with the O-$Cu^{1+}_{S=0}$-O axis tilted 28° from the *c* axis and with negative $d(c/a)/dP$. This transition corroborates with the onset of long-range antiferromagnetic order. Starting at ~23 GPa, with an initial volume reduction in $\sim|\Delta V/V_0|=0.16$, the Cu-Fe bands overlap and this leads to a $(Cu^{1+}_{S=0}Fe^{3+}_{S=5/2}) \rightarrow (Cu^{2+}_{S=1/2}Fe^{2+}_{S=2})$ interionic valence exchange in about 1/3 of the $C2/c$-$CuFeO_2$ at 27 GPa. As a result: (i) the Cu^{2+}-O becomes fourfold coordinated and is in a new crystallographic structure with space group $P\bar{3}m$, and (ii) the Néel temperature increases above twofold $[T_N(Cu^{2+}_{S=1/2}Fe^{2+}_{S=2}) \approx 2.2T_N(Cu^{1+}_{S=0}Fe^{3+}_{S=5/2})]$. This sequence of transitions is reversible with minimal hysteresis.

DOI: 10.1103/PhysRevB.81.104110 PACS number(s): 62.50.−p, 76.80.+y, 78.70.Dm

I. INTRODUCTION

With the development of diamond-anvil pressure cells during the past two decades,[1] we have witnessed many discoveries about compressed materials. The *transition-metal compounds*, Mott-Hubbard insulators,[2] and particularly the iron (Fe^{2+} and Fe^{3+}) containing oxides, have revealed major changes under pressure, including high- to low-spin transitions (spin crossovers) (Ref. 3) caused by the strong dependency of the crystal field $10Dq$ on interatomic distance *r* $[\sim 1/r^n,\ 4<n<6$ (Ref. 4)]. With pressures reaching mechanical energy densities (E_M/V) comparable to the Coulombic (E_C/V) energy density, strong *d*-*d* electronic correlations present at low pressures can break down, leading to an abrupt insulator-metal transition accompanied by the collapse of the magnetic moment.[5] In addition, we have documented pressure-induced *self-oxidation* of Fe^{2+} in $Fe(OH)_2$: $Fe^{2+} \xrightarrow{P} Fe^{3+}+e^-$, creating a one-electron band within the framework of the "oxidized" hydroxide. This valence transformation is isostructural and is not fully reversible upon decompression.[6]

In the present case, we describe a reversible *oxidation-reduction* transition in the antiferromagnetic insulator $CuFeO_2$ (delafossite) triggered by a sequence of structural phase transitions under pressure. At ambient conditions, delafossite crystallizes in the $R\bar{3}m$ structure consisting of hexagonal layers of Cu^{1+}, Fe^{3+}, and O^{2-} with a stacking sequence of *A*-*B*-*C* [*A*(Cu), *A*(O), *B*(Fe), *C*(O), *C*(Cu), *C*(O), *A*(Fe), etc.] along the *c* axis to form a layered triangular lattice (Fig. 1, inset).[7] The triangular sublattices of antiferromagnetic $Fe^{3+}(S=5/2)$ moments are separated by layers of nonmagnetic $Cu^{1+}(S=0)$ and O^{2-}. Early high-pressure x-ray diffraction studies by Zhao *et al.*[8] found no indications of structural phase transitions to 10 GPa but reported a significant increase in c/a with increasing pressure. This unusual

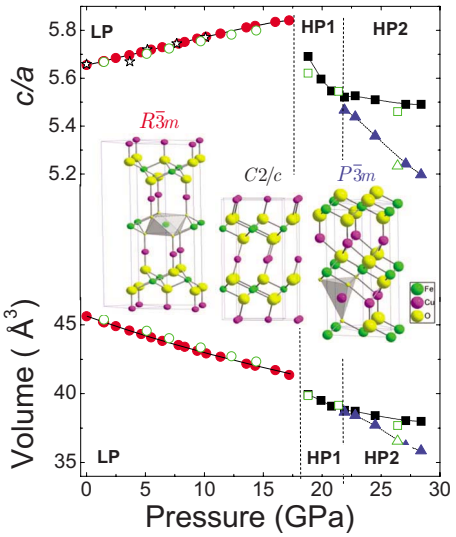

FIG. 1. (Color online) Pressure dependence of the unit-cell volume and crystal anisotropy reflected by the c/a ratio at RT. The solid line through $V(P)$ is the theoretical fit for the LP phase using the Birch-Murnaghan formula for the equation of state. Circles correspond to the $R\bar{3}m$ phase, squares to the $C2/c$, and triangles to the $P\bar{3}m$ structures. The *open* points correspond to data recorded at decompression. The stars for $c/a(P)$ are from Ref. 8. The discontinuous decrease in c/a and *V* occurs at the onset of the HP1 phase. The $R\bar{3}m$, $C2/c$, and the $P\bar{3}m$ crystal structures are shown in the inset.

pressure-induced anisotropy combined with highly frustrated spin properties both between and within layers[9] has motivated our recent ^{57}Fe Mössbauer studies to 19 GPa (Xu *et al.*[10]). Among the findings was that only for $P \geq 18$ GPa is long-range antiferromagnetic order stabilized at $T < T_N$ ($\sim$40 K at 19 GPa).

With further pressure increase an abrupt valence transition was observed by ^{57}Fe Mössbauer spectroscopy (MS) at pressures of 24–27 GPa, namely, $Fe^{3+}(S=5/2) \underset{P}{\rightleftarrows} Fe^{2+}(S=2)$, in which part of the Fe^{3+} is transformed into a new magnetic Fe^{2+} sublattice. This finding was the main motivation of the present work. In order to elucidate the nature of this pressure-induced *reduction* in a large fraction of the Fe^{3+} ions, we carried out additional ^{57}Fe Mössbauer studies, x-ray diffraction (XRD) studies, and x-ray absorption spectroscopy (XAS) at the Fe and Cu K edges, the latter to test the possibility of a concurrent $Cu^{1+}(S=0) \underset{P}{\rightleftarrows} Cu^{2+}(S=1/2)$ transition. The combined methods lead to a comprehensive portrayal of the high-pressure phases of $CuFeO_2$.

II. EXPERIMENTAL

$CuFeO_2$ was synthesized by direct solid-solid reaction of Fe_2O_3 and Cu_2O.[11] Mössbauer samples were prepared with Fe_2O_3 enriched in 20% of ^{57}Fe. XRD and XAS were carried out at room temperature (RT) and the MS in the 5–300 K range and pressures to 30 GPa. Pressure was generated with *opposing plates* diamond-anvil cells using anvils with 300 μm culets. Argon or helium was used as a pressurizing medium.

Mössbauer studies were performed using a ^{57}Co (Rh) point source in a variable temperature (5–300 K) cryostat. Spectra were analyzed using a spin-Hamiltonian fitting program assuming $e^2 q_{zz} Q/4I(2I-1) \ll \mu H_{hyp}/I$ from which the isomer shift (IS), the quadrupole splitting (QS), the hyperfine field (H_{hf}) and the relative abundances of the spectral components were deduced. Due to the high ^{57}Fe isotopic enrichment (20%) typical line widths were as high as 0.35 mm/s.

XRD was performed in angle-dispersive mode at the ID09A beamline of the European Synchrotron Radiation Facility, Grenoble, with patterns collected using a MAR345 detector and integrated using the FIT2D program.[12] Two sets of measurements were obtained, using wavelengths $\lambda = 0.41761$ and 0.41336 Å, and the results analyzed by Rietveld refinement using the GSAS package.[13]

XAS was performed at the energy-dispersive beamline ID24 of ESRF employing a Si(220) polychromator and three Si mirrors for harmonic rejection and vertical focusing.[14] The focal spot was $\sim 5 \times 5$ μm full width at half maximum and use of partially perforated anvils[15] substantially reduced absorption of the Cu and Fe K x rays by the diamonds. The results were analyzed through comparison with x-ray spectra calculated using the *ab initio* self-consistent real-space multiple-scattering code FEFF8.4.[16] An energy-dependent exchange-correlation Hedin-Lundqvist potential was used within the muffin-tin approximation, and self-consistency was obtained by successively calculating the electron density of states, electron density and Fermi level within a cluster of 50 atoms and then iterating. Full multiple-scattering calculations up to photoelectron energy of about 60 eV were carried out for a larger cluster of 150 atoms centered on the photoabsorber, and a constant experimental broadening of 0.5 eV and an offset in the energy scale of −5.5 eV were added.

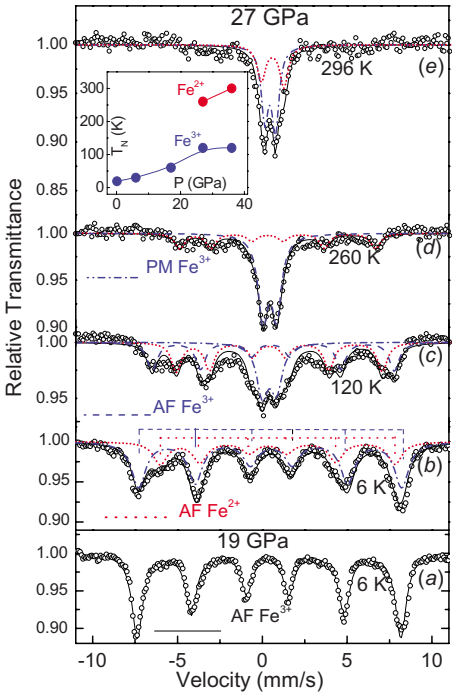

FIG. 2. (Color online) Mössbauer spectra of $CuFeO_2$ recorded at 19 and 27 GPa: typical absorption spectrum of the 19–23 GPa range ($C2/c$ structure) at 6 K (a) characterized by a single magnetic Fe^{3+} component with parameter values within the range observed for ferric oxides. Spectra typical for 24–30 GPa range recorded at various temperatures are shown in (b)–(e). The fitted solid line through the experimental points is a convolution of two spectral components: At 6 K (b) the spectrum is composed of two magnetic components: Fe^{3+} and a new one with H_{hf} and IS characteristic of Fe^{2+} oxides; (c) at 120 K one observes the collapse of the magnetic order of the Fe^{3+} component, showing a central peak representing the fast spin-spin relaxation typical of the $T \sim T_N$ regime; at 260 K (d) the Fe^{2+} magnetic splitting is still observed *albeit* with reduced H_{hf}(=36 T); and at RT (e) the paramagnetic quadrupole-split components of Fe^{3+} and Fe^{2+} are the only ones left. The solid line is a result of fitting to two quadrupole-split components (Fe^{3+} and Fe^{2+}) with relative abundance of 2/1 (Ref. 26). The inset summarizes the $T_N(P)$ of the two Fe species, Fe^{3+} and Fe^{2+}.

III. RESULTS AND DISCUSSION

Typical Mössbauer spectra recorded at 19–23 GPa range at 6 K and at 24–30 GPa range in the 5–300 K range are shown in Fig. 2. The 19 GPa spectrum corresponds to a single-site Fe^{3+} magnetic hyperfine field (H_{hf}) of 48(2) T with IS=0.34(2) mm/s.[17] T_N at this pressure is 38(3) K as obtained from a series of $H_{hyf}^{19\ GPa}(T)$ measurements.[10] With

increasing pressure, above 24 GPa, a new magnetic hyperfine component appears with parameters values [IS =0.63(2) mm/s and H_{hf}=42(2) T] that can be unambiguously attributed to a high-spin Fe^{2+} (Ref. 18) at such pressures. With increasing temperature H_{hf}(T) values of both components decrease, signaling the decrease in magnetization of both species while approaching their corresponding T_N. At 120 K, the quadrupole-split paramagnetic component attributed to paramagnetic relaxation of Fe^{3+} (centered at $v \sim 0$ mm/s), is typical of the $T \sim T_N$ regime at high pressure (see, for example, Ref. 3); and at 260 K the only *magnetic component* remaining is that of Fe^{2+} with H_{hf} =36(2) T whereas the quadrupole-split central component originates from paramagnetic Fe^{3+} with a Fe^{3+}/Fe^{2+} abundance ratio of 2/1. Finally, at room temperature (T_N <300 K), both the ferric and ferrous quadrupole-split components are paramagnetic with QS(Fe^{3+})=0.72(2) mm/s, IS(Fe^{3+})=0.39(2) mm/s, QS(Fe^{2+})=1.00(2) mm/s, and IS(Fe^{2+})=0.61(2) mm/s. T_N of both iron species increase with pressure (inset in Fig. 2), typical for antiferromagnetic *Mott-Hubbard* insulators. Thus we infer that above 24 GPa two Cu-Fe species are present: $Cu^{1+}Fe^{3+}O_2$ [T_N =130(10) K] and $Cu^{2+}Fe^{2+}O_2$ [T_N=280(20) K], the latter composed of two magnetic sublattices, $Cu^{2+}(S=1/2)$ and $Fe^{2+}(S=2)$. Mössbauer spectra obtained with reducing pressure showed no hysteresis suggesting that electronic/magnetic pressure-induced transitions are reversible.

XRD patterns obtained at various pressures are shown in Fig. 3. Up to 18 GPa, the low-pressure (LP) regime, spectra are well fitted assuming the ambient-pressure space group $R\bar{3}m$.[8] A spectrum typical of this phase is shown in Fig. 3(a). At $P \approx 18$ GPa a first-order transition takes place characterized by a symmetry change, volume and c axis drop and reversal of the c/a slope. Within the 18–22 GPa range the diffraction patterns are satisfactorily fitted with space group $C2/c$ [Fig. 3(b)] with the weighted residual and residual agreement factors $wRp < 1.3\%$ and $Rp < 1\%$, respectively.[19] This phase is designated as the *high-pressure 1* (HP1) phase. Similar to $R\bar{3}m$ it is also a layered hexagonal structure that is obtained by layers displaced in the ab plane, resulting in a tilt of the rigid O-Cu-O "dumbbells" by ~28° relative to the c axis (Fig. 1). Above 22 GPa domains of an additional structure appear arising from the $C2/c$ structure, as evident from splitting of the (004) peak and broadening of other peaks except ($hk0$) [Fig. 3(c)]. This partial transformation can be explained by an additional displacement of part of the Cu and O layers in the ab plane resulting in a different stacking sequence to form $P\bar{3}m$ domains (see Fig. 1) coexisting with $C2/c$ domains. This new phase is designated as the *high-pressure 2* (HP2) phase, in which $CuFeO_2$ is comprised of $P\bar{3}m$ and $C2/c$ clusters. Patterns of the HP2 phase were correspondingly fitted with this assumption and the quality of the fitting can be appreciated by the derived small values of wRp(<1.1%) and Rp(<0.7%).

The derived $V(P)$ and $(c/a)(P)$ graphs are shown in Fig. 1. The $V(P)$ data for the LP phase (Fig. 1) are well fitted with a second-order Birch-Murnaghan equation[20] with the following parameters: K_0=148.0(0.7) GPa, K_0'=4 (fixed), and V_0 =45.64(0.01) Å^3, where K_0, K_0', and V_0 are the bulk modulus, its pressure derivative, and the unit-cell volume at ambient conditions, respectively. As can be seen, $(c/a)(P)$ increases beyond 10 GPa, the last pressure point measured by Zhao *et al.*,[8] culminating at 18 GPa with a total increase of ~3% with respect to ambient pressure. This large increase in anisotropy is evidently unstable, and at $P > 18$ GPa a structural LP→HP1 phase transition takes place accompanied by a discontinuous volume decrease ($\Delta V/V_{18\ GPa} \sim 0.03$), increase in dV/dP, a large drop in c/a and a reversal in its pressure derivative from positive to negative, signaling the collapse of the high axial anisotropy in $CuFeO_2$. Within the HP1 $C2/c$ phase, the 28° tilt of the O-Cu-O bonds with respect to the c axis apparently exposes the CuO_2 to soft

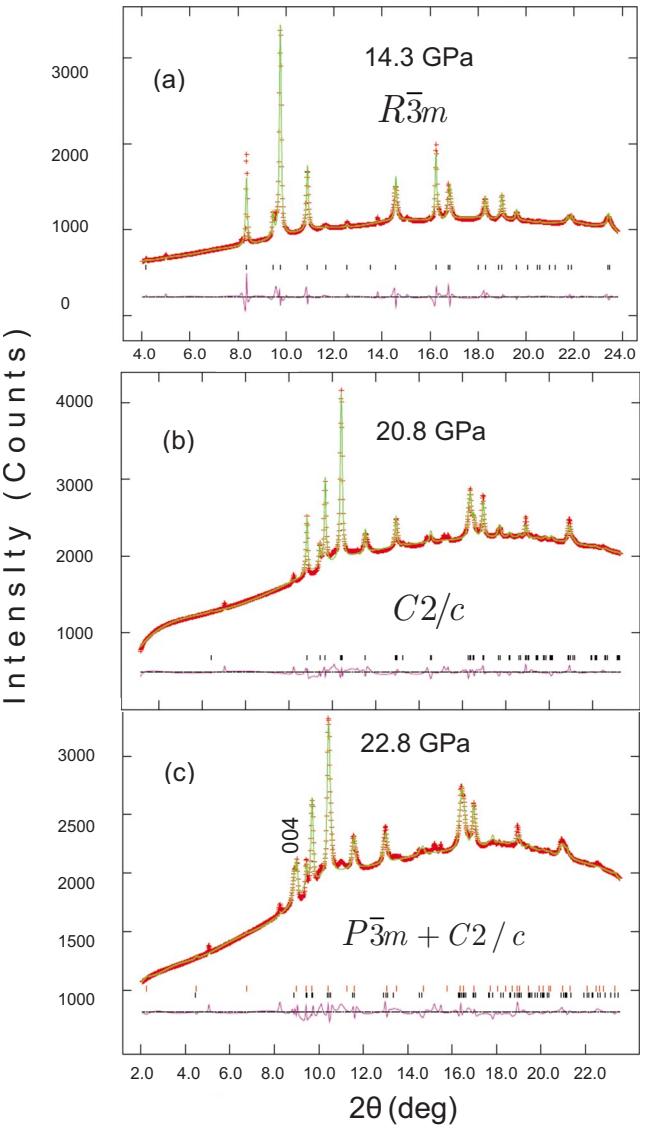

FIG. 3. (Color online) Typical examples of analyzed integrated patterns of XRD spectra collected at 14.3, 20.8, and 22.8 GPa at RT and the differences between the observed and calculated profiles. Marks show the calculated peak positions. The 14.3 GPa spectrum corresponds to the LP phase with $R\bar{3}m$ symmetry, extending from ambient pressure to 18 GPa. At 19–22 GPa the symmetry group is $C2/c$ and at $P > 22$ GPa $CuFeO_2$ is comprised of both $C2/C$ and $P\bar{3}m$ domains.

TABLE I. The Fe-O and Cu-O mean value distances (Å) at various pressures within the $R\bar{3}m$, $C2/c$, and the $P\bar{3}m$ phases.

P (GPa)	Fe-O	Cu-O
	$R\bar{3}m$ phase ($Cu^{1+}Fe^{3+}O_2$)	
1.4	2.033(5)	1.815(1)
6.4	2.010(4)	1.809(1)
11.4	1.991(4)	1.805 (1)
17.2	1.970(2)	1.799(4)
	$C2/c$ phase ($Cu^{1+}Fe^{3+}O_2$)	
18.8	1.967(1)	1.901(1)
21.9	1.952(2)	1.855(2)
24.5	1.946(1)	1.847(1)
28.4	1.939(1)	1.838(1)
	$P\bar{3}m$ phase ($Cu^{2+}Fe^{2+}O_2$)	
21.9	2.057(3)	1.944(3)
24.5	2.041(1)	1.925(1)
28.4	2.008(8)	1.887(7)

bending modes, causing a reduction in c/a values and bulk modulus as compared with the $R\bar{3}m$ structure. This structural phase transition stabilizes the long-range antiferromagnetic order[21] but has no observable effect on the valence state of Fe as evident from the Mössbauer spectra.

With further pressure increase and consequent volume decrease in $CuFeO_2$ in its $C2/c$ configuration, $Cu^{1+}(3d^{10})$ and $Fe^{3+}(3d^5)$ bands overlap at $\sim|\Delta V/V_0|=0.16$ (23 GPa) resulting in an intercationic charge exchange, and leading to a valence transformation in parts of the Cu and Fe constituents: $Cu^{1+}(\rightarrow Cu^{2+})$ and $Fe^{3+}(\rightarrow Fe^{2+})$.[22] The $Cu^{1+}\rightarrow Cu^{2+}$ transition, particularly, has dramatic consequences for the stability of the $C2/c$ phase, with an onset of Cu^{2+}-O bonding with fourfold coordination instead of the twofold O-Cu-O dumbbell-like bonding. The four-coordinated Cu^{2+} species cannot be accommodated within the $C2/c$ framework, and as a result, domains of the $P\bar{3}m$ structure appear characterized by the formation of tetrahedral CuO_4 distorted along the c direction (see Fig. 1). Accordingly, at the HP1-HP2 boundary $V(P)$ and $(c/a)(P)$ branch into two curves corresponding to the $P\bar{3}m$ and $C2/c$ domains.

Typical Fe-O and Cu-O mean value distances for the $R\bar{3}m$, $C2/c$, and the $P\bar{3}m$ phases as obtained from the XRD results are shown in Table I. It is noteworthy that the Fe-O distances differ within the $C2/c$ and $P\bar{3}m$ structures, for the same pressure values, although Fe remains sixfold coordinated: the larger Fe-O distance in the $P\bar{3}m$ phase is consistent with the larger ionic radius of Fe due to the $Fe^{3+}\leftrightarrow Fe^{2+}$ valence transformation. The larger value of the Cu-O distance in the $P\bar{3}m$ phase with respect to the $C2/c$ phase results from the combined effect of the expansion of the Cu-O bond due to the Cu coordination change from 2 ($C2/c$) to 4 ($P\bar{3}m$), and of the slight contraction of the Cu ionic radius due to the $Cu^{1+}\leftrightarrow Cu^{2+}$ valence transformation.[23]

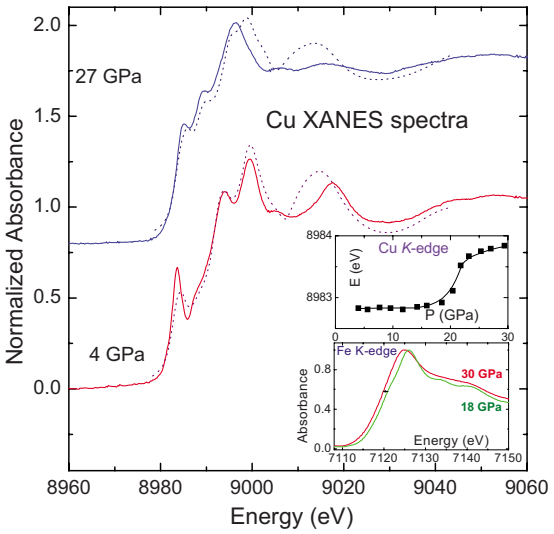

FIG. 4. (Color online) XANES spectra at Cu K edge at RT. Simulations (dotted lines) were based on the assumption of the $R\bar{3}m$ space group for the data at 4 GPa, and of a coexistence of $C2/c$ and $P\bar{3}m$ with an abundance ratio of 2:1 for the data at 27 GPa. The top inset shows the energy of the Cu K-edge absorption onset as a function of pressure. The bottom inset shows Fe K-edge spectra at 18 and 30 GPa. With the appearance of Cu^{2+} the Cu K-edge absorption onset increases by ~1 eV, whereas the Fe K-edge absorption onset shows a negative shift of comparable magnitude.

Cu K-edge x-ray absorption near-edge structure (XANES) spectra are shown in Fig. 4. We compare the normalized experimental data (continuous line) to *ab initio* simulations (dotted line) based on the $R\bar{3}m$ phase for the data at 4 GPa (bottom) and on a combination of $C2/c$ and $P\bar{3}m$ phases with 2:1 relative abundance for the data at 27 GPa (top). Upon pressure increase, the modifications of the spectral features close to the absorption edge are well reproduced by the simulations. The Cu absorption edge shifts by about +1 eV in the 20–30 GPa range, whereas the iron edge exhibits a negative shift (see insets in Fig. 4). Given that within the family of pure iron and copper oxides the energy of the x-ray absorption edge increases with increasing valence at constant pressure,[24,25] our XANES data are consistent with a valence transformation $Cu^{1+}\rightarrow Cu^{2+}$ and $Fe^{3+}\rightarrow Fe^{2+}$ in part of the Cu and Fe sites. Thus, the x-ray spectroscopic and diffraction results support our interpretation of the Mössbauer data as reflecting the following electronic transition,

$$[Cu^{1+}_{(S=0)}Fe^{3+}_{(S=5/2)}O_2] \xrightarrow{P\geq 23\ \text{GPa}} x[Cu^{2+}_{(S=1/2)}Fe^{2+}_{(S=2)}O_2] + (1-x) \times [Cu^{1+}_{(S=0)}Fe^{3+}_{(S=5/2)}O_2]. \quad (1)$$

The appearance of Cu^{2+} ($3d^9, S=1/2$) paramagnetic sublattices significantly affects the magnetic properties of $CuFeO_2$ above 22 GPa: the "weak" $Fe^{3+}_{S=5/2}$-O-$Cu^{1+}_{S=0}$-O-$Fe^{3+}_{S=5/2}$ superexchange paths are replaced by a "robust" $Fe^{2+}_{S=2}$-O-$Cu^{2+}_{S=1/2}$-O-$Fe^{2+}_{S=2}$ superexchange, composed now of a

paramagnetic Cu^{2+} sublattice and leading to an enhanced T_N that jumps more than twofold (from 130 to 280 K) at 27 GPa. With further pressure increase, $T_N^{P\bar{3}m}(P)$ increases rapidly and reaches 300 K at 36 GPa whereas $T_N^{C2/c}(P)$ barely changes (Fig. 2, inset). This can be explained as due to the higher compressibility of the $P\bar{3}m$ phase in comparison with the $C2/c$ phase (see Fig. 1).

IV. CONCLUSIONS

In conclusion, the observed series of intertwined structural, electronic, and magnetic changes in $CuFeO_2$ include the structural instability of the $R\bar{3}m$ lattice beyond 18 GPa, resulting in a more stable $C2/c$ structure. Above 23 GPa part of the $C2/c$ transforms into $P\bar{3}m$ structure in which Fe-Cu intersite charge transfer occurs. This series of transitions may not be completed at the HP2 phase (comprised of $P\bar{3}m$ and $C2/c$ domains). It can be expected that with further pressure increase $CuFeO_2$ will be fully transformed to $P\bar{3}m$ or to another energetically stable structure. The observed *intersite* charge transfer is accompanied by considerable changes in the material's elastic and magnetic properties, and the transitions are completely reversible with no noticeable hysteresis in pressure.

ACKNOWLEDGMENTS

This research was supported in part by Israeli Science Foundation under Grant No. 36/05, and the U.S. Department of Energy and National Science Foundation. Part of the experiments was performed at the Bayerisches Geoinstitut under the EU "Research Infrastructures: Transnational Access" Program [Contract No. 505320 (RITA), High Pressure]. We thank Y. Amiel, E. Greenberg and R. Arielly for assisting with the XRD and XAS measurements.

[1] R. J. Hemley and N. W. Ashcroft, Phys. Today **51** (8), 26 (1998); R. J. Hemley, Annu. Rev. Phys. Chem. **51**, 763 (2000).

[2] N. F. Mott, *Metal-Insulator Transitions* (Taylor & Francis, London, 1990), and references therein.

[3] W. M. Xu, O. Naaman, G. K. Rozenberg, M. P. Pasternak, and R. D. Taylor, Phys. Rev. B **64**, 094411 (2001).

[4] P. García-Fernández, J. M. García-Lastra, J. A. Aramburu, M. T. Barriuso, and M. Moreno, Chem. Phys. Lett. **426**, 91 (2006).

[5] M. P. Pasternak, R. D. Taylor, A. Chen, C. Meade, L. M. Falicov, A. Giesekus, R. Jeanloz, and P. Y. Yu, Phys. Rev. Lett. **65**, 790 (1990).

[6] M. P. Pasternak, A. P. Milner, G. K. Rozenberg, R. D. Taylor, and R. Jeanloz, Phys. Rev. Lett. **92**, 085506 (2004).

[7] M. Hasegawa, M. I. Batrashevich, T. R. Zhao, H. Takei, and T. Goto, Phys. Rev. B **63**, 184437 (2001).

[8] T. R. Zhao, M. Hasegawa, T. Kondo, T. Yagi, and H. Takei, Mater. Res. Bull. **32**, 151 (1997).

[9] P. Fazekas and P. W. Anderson, Philos. Mag. **30**, 423 (1974).

[10] W. M. Xu, M. P. Pasternak, and R. D. Taylor, Phys. Rev. B **69**, 052401 (2004).

[11] Polycrystalline samples were prepared by thoroughly grinding and mixing of stoichiometric proportions of Cu_2O and Fe_2O_3. The oxide mixture was pressed into discs and fired at 900 °C for 24 h after which it was quenched to room temperature. All firing and quenching were performed in a nitrogen atmosphere.

[12] A. P. Hammersley, computer program FIT2D, ESRF, Grenoble, 1998.

[13] A. C. Larson and R. B. Von Dreele, Los Alamos National Laboratory Report No. LAUR 86, 1994 (unpublished).

[14] S. Pascarelli, O. Mathon, M. Munoz, T. Mairs, and J. Susini, J. Synchrotron Radiat. **13**, 351 (2006).

[15] Supplied by D'Anvils Ltd.

[16] A. L. Ankudinov, A. I. Nesvizhskii, and J. J. Rehr, Phys. Rev. B **67**, 115120 (2003).

[17] IS values are with respect to α iron at 300 K. ^{57}Co (Rh) source was at the same temperature as the absorber.

[18] The IS and H_{hf} of the Fe^{3+} component at this pressure were 0.39(2) mm/s and 48(2) T, respectively.

[19] $Rp=\Sigma|I_o-I_c|/\Sigma I_o$ and $wRp=\mathrm{sqrt}\{\Sigma w(I_o-I_c)^2)/\Sigma wI_o^2\}$, where I_o and I_c are observed and calculated profile values. For more details see Ref. 13.

[20] O. L. Anderson, *Equations of State of Solids for Geophysics and Ceramic Science* (Oxford University Press, Inc., New York, 1995).

[21] Noteworthy that at ambient pressure on cooling from room temperature, $CuFeO_2$ undergoes antiferromagnetic transition at 11 K which is accompanied by structural phase transitions to monoclinic $C2/m$ structure [F. Ye, Y. Ren, Q. Huang, J. A. Fernandez-Baca, Pengcheng Dai, J. W. Lynn, and T. Kimura, Phys. Rev. B **73**, 220404 (2006)]. In contrast to the present case only slight monoclinic distortion of the original hexagonal $R\bar{3}m$ structure is observed in this case.

[22] We note that there is a slight difference in determining the pressure limits of HP1 and HP2 between the XRD and MS studies. Differences may arise from the higher sensitivity of the synchrotron XRD method, where the higher signal/noise allows detection of new components at a level where its relative abundance is too small for MS. The different geometry of the signal collection also can play a role: the pressure is measured usually in the center of the hole, in the XRD measurements the signal derives also from a small central part of the sample, whereas in MS studies the signal is collected from a larger part of the sample ($\sim 2/3$) resulting in possible pressure gradient effects.

[23] According to R. D. Shannon, Acta Crystallogr., Sect. A **32**, 751 (1976) the ionic radii at ambient conditions of Fe^{2+}(VI) and Fe^{3+}(VI) are 0.78 Å and 0.645 Å and of Cu^{2+}(IV) and Cu^{1+}(II) are 0.57 Å and 0.46 Å, respectively.

[24] The Fe *K*-edge position moves toward higher energies with increasing Fe valence within the family of iron oxides FeO, Fe_2O_3, and Fe_3O_4: see M. Newville, S. A. Carroll, P. A. O'Day, G. A. Waychunas, and M. Ebert, J. Synchrotron Radiat. **6**, 276 (1999).

[25] K. Akeyama, H. Kuroda, and N. Kosugi, Jpn. J. Appl. Phys., Suppl. **32**, 98 (1992).

[26] The two doublet components are slightly asymmetric due to the texture effect induced by pressure.